Network-Constrained Rail Transportation and Power System Scheduling with Mobile Battery Energy Storage Under a Multi-Objective Two-Stage Stochastic Programming

Mohammad Amin Mirzaei[1], Mohammad Hemmati[1], Kazem Zare[1], Behnam Mohammadi-Ivatloo[1], Mehdi Abapour[1], Mousa Marzband[2], Reza Razzaghi[3], Amjad Anvari-Moghaddam[4,1]

[1]Faculty of Electrical and Computer Engineering, University of Tabriz, Tabriz, Iran

[2]Department of Mathematics, Physics and Electrical Engineering, Northumbria University, Newcastle, England

[3]Department of Electrical and Computer Systems Engineering, Monash University, Clayton VIC 3800, Australia

[4]Department of Energy Technology, Aalborg University, 9220 Aalborg, Denmark

Abstract

By increasing environmental pollution and the energy crisis, the development of renewable energy sources (RESs) has become an essential option to ensure a sustainable energy supply. However, the inherent uncertainty of RESs poses significant technical challenges for independent system operators (ISOs). Transmission line congestion has become one of the significant challenges for ISOs to use the maximum power of RESs. The mobile battery-based energy storage systems can provide a promising solution for the transportation of the generated energy from RESs to load centers to mitigate the effects of line congestion on the power network operation. Hence, this paper evaluates the impact of battery-based energy storage transport by a train called BESTrain in a unit commitment model from the economic, environmental, and technical aspects under a multi-objective mixed-integer linear programming framework. The uncertainties associated with wind power and electric demand are also handled through a two-stage stochastic technique. The main aim of the introduced model is to minimize the carbon emission and operational cost simultaneously by determining the hourly location and optimal charge/discharge scheme of the BESTrain, and optimal scheduling of power plants. The numerical results exhibit the reduction of operation cost and carbon emission by 6.8% and 19.3%, respectively, in the presence of the BESTrain.

Keywords: Railway transport network, battery-based energy storage transport, multi-objective optimization, vehicle routing problem, stochastic programming, wind energy.

NOMENCLATURE

Index

b, b'	Buses
i	Power plants
j	Loads
k, n	Train station
m	Production blocks
t	Time periods
ts	Time spans
tr	Trains
s	Scenarios
wp	Wind power plants

Constant

$CE_{i,t}$	Carbon emission coefficient of power plants
η_{tr}^{ch} / η_{tr}^{dis}	Charge/discharge efficiency of trains
$voll_{j,t}$	Cost of lost load
$D_{j,t,s}$	Electrical demands
$C_{i,t,m}^{E}$	Energy prices offered by power plants
$E_{tr,0}$	Initial energy level of trains
$X_{b,b'}$	Line reactance
$PF_{Line}^{\max}$	Maximum thermal capacity of the transmission line
$E_{tr}^{\min}$ / $E_{tr}^{\max}$	Min/max capacity for train*s*
$P_{tr}^{ch,\min}$ / $P_{tr}^{ch,\max}$	Min/max charge power of trains
$P_{tr}^{dis,\min}$ / $P_{tr}^{dis,\max}$	Min/max discharge power of trains
$P_{i}^{\min}$ / $P_{i}^{\max}$	Min/max power produced by power plants
$ME_{i,t}$	Minimum carbon emission produced by plants
MUT_i / MDT_i	Minimum down/up times for power plants
$MC_{i,t}$	Minimum operation cost of power plants
π_s	Scenario probability

C_i^{SU} / C_i^{SD}	Start-up/shut-down costs for power plants
A	Sum of arcs for time-space network
A_k^+	Sum of arcs in a time-space that starts from *k* station
A_k^-	Sum of arcs in TSN that end at *k* station
J	Sum of electrical loads
M	Sum of generation blocks
NJ	Sum of loads
U	Sum of power plants
N	Sum of power plants
S	Sum of second stage scenarios
T	Sum of time intervals
TS	Sum of time-spaces
TR	Sum of train
TR	Sum of trains
WP	Sum of wind power plants
$P_{wp,t}$	The produced wind power
C_{tr}^{ch}	Trains operation cost in charging mode
C_{tr}^{dis}	Trains operation cost in discharging mode
C_{tr}	Transportation cost for trains
R_i^{up} / R_i^{down}	Up and down ramp of power plants

Variable

$\Delta P_{tr,t,s}^{ch}$	Adjusted charging power by BESTrains
$\Delta P_{tr,t,s}^{dis}$	Adjusted discharging power by BESTrains
$\Delta PE_{i,t,s}$	Adjusted carbon emission by power plants
$\Delta P_{i,t,m,s}$	Adjusted power of power plants
$\theta_{b,t}$	Angle magnitude of bus *b* at time *t*
$PE_{i,t}$	Carbon emission of power plants
$P_{tr,t}^{ch}$ / $P_{tr,t}^{dis}$	Charge/discharge power of trains
$TU_{i,u}$ / $TD_{i,u}$	Number of successive ON/OFF hours for power plants
$PF_{b,b',t}$	Power flow of lines between buses
$P_{i,t}$	Power production of power plants
$SU_{i,t}$ / $SD_{i,t}$	Start-up/shut-down cost of power plants

$E_{tr,t}$ The energy capacity of trains

$Lsh_{j,t}$ Value of lost load at *t* time

$\Theta_{j,t,s}$ Variable amount $\Theta \in \{D, Lsh\}$ in the second stage

$\Theta_{tr,t,s}$ Variable amount $\Theta \in \{E^r, P^{ch,r}, P^{dis,r}\}$ in the second stage

$\Theta_{i,t,s}$ Variable amount $\Theta \in \{P^r, PE^r\}$ in the second stage

$\Theta_{b,t,s}$ Variable amount $\Theta \in \{PF^r, \theta^r\}$ in the second stage

Binary variables

$Y_{i,t} / Z_{i,t}$ Binary variable for start-up/shut-down of power plants

$I_{i,t}$ Binary variable for the status of power plants

$F_{tr,k,n,ts}$ Status of route *k-n* of train *tr* at time span *ts*

$I^{ch}_{tr,t} / I^{dis}_{tr,t}$ Binary variable of charge/discharge operation mode of trains

1. Introduction

A. Motivation

The total global share of wind energy is projected to reach 36% by 2030 [1]. The unpredictable power generated by wind energy could expose adverse effects on the optimal operation of power systems. In addition to power fluctuations, the most important challenge in developing wind power plants is the transfer of power generated by such power plants from production to consumption through high-cost transmission lines [2]. Therefore, keeping a balance between generation and consumption with high wind energy penetration in the power grid is fundamental. Battery energy storage systems (BESSs), as flexible emerging technologies with unique features such as mobility and high efficiency, can present an appropriate solution to mitigate challenges associated with wind power variability [3, 4]. Mobility can be considered as one of the unique features of BESS. This feature makes it easy to carry BESS across the network under different conditions. The mobile BESSs provide an appropriate solution to transport the generated wind energy from wind farms sides to load centers all over the power system. The rail transport networks (RTNs) cover a large part of the transportation system worldwide for daily passengers traveling. However, installing BESS in train carriages provides a suitable opportunity to take advantage of battery mobility. The battery-based energy storage transport via a train called BESTrain can overcome wind power transmission challenges

from the generation side to consumption centers by relieving congestion difficulties in transmission lines during peak hours.

B. Literature review

Several studies focused on renewable energy sources integration management using flexible emerging technologies. A two-stage stochastic unit commitment (UC) model was presented in [5] to evaluate the bulk energy storage (BES) capacity incorporated with wind energy on the daily operation cost. In [6], a UC model incorporated with the large-scale BESS and renewable energy resources was proposed by considering the degradation cost of BESS and load uncertainty. A new model for calculating the technical and economic flexibility criterion of the power grid was proposed in [7] by considering BESS and demand response (DR) resources. The economic-emission evaluation of DR and parking-lot electric vehicle (PEV) was studied in [8] under a multi-objective UC model. In [9], a bi-level optimization problem was proposed, where the BESS is considered as a price-maker player in the power market. A comprehensive study of the role of DR in energy and storage markets was conducted in [10] as a multi-objective optimization framework to reduce wind energy fluctuations and minimize operating costs. A new model for optimal energy and reserve scheduling of the modern power systems considering BES, DR, and wind energy was investigated in [11]. In [12], the relationship between wind curtailment value and operation cost using multi-objective UC integrated with BESS was evaluated, where the impacts of BESS on the uncertainty management and load shedding are evaluated. A probabilistic UC model combined with BESS was studied by [13], where the Benders decomposition method is applied to solve it and reduce the computational burden. A stochastic UC problem for a hybrid micro-grid in the presence of wind and solar energies and BESS considering load forecasting error was developed by [14], aiming to minimize total operation cost. The authors of [15] introduced an emerging BESS as part of the set of control measures in a corrective form of the UC model under a two-stage MILP formulation applying the Benders decomposition approach.

The energy storage system has been studied as a fixed technology (static storage) in renewable-based power grids in the mentioned literature. Meanwhile, one of the most obstacles of wind power is too much distance

between distribution networks and wind farms. Hence, the high value of wind power inevitably interrupted to prevent the congestion of lines. For example, the curtailment rate of wind energy has grown up to 5% in Germany and 6% in Britain (for offshore and onshore Scottish wind farms) [16]. BESS mobility provides a convenient solution for transferring wind energy from production (wind farms or coastal farms) to consumption, thereby reducing the challenges of integrating wind farms into the power grid. However, providing the necessary infrastructures for the BESS transferring has rarely been developed in the literature. A UC model incorporated with the BESS transportation was studied by [17], where the role of BESTrain on the daily operation cost and congestion of lines is investigated without considering system uncertainties. In [18], the restoration of joint post-disaster scheduling of the distribution system, including neighboring micro-grids incorporated with the transportable BESS, was extended. The shipping, trains, and trunks infrastructures for extending the potential of the BESTrain to mitigate congestion challenges related to the transmission system was developed by [19], where a UC model coordinated with BESTrain is solved. The effect of BESTrain on the optimal scheduling of power plants under a UC model was studied in [20], where a stochastic time-space network (TSN) model is adopted to handle the stochastic nature of the railway system. A multi-agent system-based strategy for service restoration in a distribution network with power plants and mobile energy storage systems was proposed in [21], where a three-layer structure is introduced to consider cyber, physical, and transportation layers. The authors of [22] investigated the effect of the mobile battery storage system in distribution networks, where the optimal location and charge and discharge scheme of the battery storage system are determined during the scheduling period. The authors of [23] evaluated the effect of EVs on the transmission-constraints UC model to mitigate the wind power fluctuation in the power system. The scenario-based stochastic UC model incorporated with EV fleet capturing load, wind output, and arrival/departure times of EV uncertainties was studied in [24]. The probabilistic UC model coordinated with the EV fleet in the presence of wind power was proposed in [25], where the traffic system is modeled by EVs traveling.

The need to utilise green and pollution-free technologies, such as hybrid BESS and wind energy, is critical due to the increasing carbon emission and climate change challenges. Techno-economic analysis of BESS

for wind energy integration, considering both technical and environmental constraints, was developed by [26]. Multi-objective optimization of BESS with large-scale integration of renewable energy considering economic and environmental constraints was investigated by [27]. The stochastic multi-objective economic/environmental operation of a micro-grid in the presence of BESS was studied in [28], where a hybrid meta-heuristic algorithm based on differential evolution (DE) and modified particle swarm optimization (PSO) is applied to solve the proposed problem. The multi-objective operation of multi-energy micro-grids in the presence of the BESS and DR program, aiming to minimize total operation cost and emission pollution, was developed by [29]. Techno-economic and environmental evaluation of BESS under multiple time scales capturing price variation was investigated by [30]. The energy management of smart homes incorporated with small-scale wind turbines and BESS under the techno-economic assessment was investigated by [31], where the proposed model determines the optimal BESS capacity. The multi-objective MILP model of home energy management problem integrated with BESS to minimize electricity bid and peak demand for multiple residential consumers was developed by [32]. In [33], an environmental/economic assessment for optimal energy management of renewable-based micro-grid incorporated with battery and photovoltaic system, and wind energy under high-level uncertainty of power price and RES was investigated. A new two-step approach was presented in [34] for obtaining the optimal BESS sizing in a grid-connected micro-grid with the aim of total operation cost reduction. In [35], a mixed-integer linear programming (MILP) model for BESS operation in distribution networks considering network losses and voltage magnitudes was developed, where the BESS exchange not only active power but also provides reactive power through inverter-based connection.

C. Gaps and Contributions

To the best knowledge of the authors, the studied works have not comprehensively explored the technical, environmental, as well as economic advantages of BESTrain in a multi-objective two-stage UC model. The remarkable gaps in the literature are outlined as follows:

- In [5-15], BESSs have been applied as static sources into power systems for multiple goals, and the mobility capability of BESS in decreasing lines congestion and minimizing operational cost in the transmission-constrained scheduling has been neglected.
- In [16-22], although the mobility capability of BESS has been deployed in the UC, they have not comprehensively investigated economic, technical environmental assessment of BESTrain under a multi-objective framework.
- In [23-32], although power systems operation has been incorporated with static or mobile BESS, the optimal UC model has not been achieved based on multi-objective approaches to capture both economic and environmental benefits.
- In [26-36], although the optimal scheduling of energy storage in the power system has been evaluated from economic, technical, and environmental perspectives, the integration of the BESTrain in the UC model in the presence of high penetration of wind energy based on the multi-objective approach have not been studied.

This work presents a multi-objective two-stage stochastic UC model for coordinated power and railway transportation networks to cover the above gaps. The proposed model enhances the flexibility of the power system via BESTrain, aiming to minimize total operational cost and emission. The BESTrain facilitates the integration of wind power into the electricity grid by transferring power from generation to consumption through the train, thereby reducing the impact of lines congestion on the optimal scheduling of power plants during peak-hours. In the proposed model, the BESTrain owner sends the price-quantity values and technical specifications to the independent system operator (ISO). Then the ISO solves the multi-objective UC problem by considering the vehicle routing problem (VRP). In VRP, a TSN is adopted to model all RTN constraints and its interdependency on the power system to achieve a more realistic RTN and power network model. After solving the UC problem, the charge and discharge schedule of the BESTrain and its hourly location and state are determined in a day-ahead scheduling model, and the BESTrain owner acts according to the pre-specified schedule. The proposed two-stage UC multi-objective optimization framework is formulated as a MILP model to capture the technical, environmental, and economic

advantages of BESTrain. Also, a scenario-based stochastic method is used to address uncertainties caused by load and wind power fluctuations. The novelty and contributions of this work are outlined as follows:

- The VRP-based BESTrain model is incorporated into the UC problem, which combines rail transport and power network constraints for optimal scheduling of power and transport systems.
- In this work, the influence of BESTrain on the hourly dispatch of power plants, locational marginal price (LMP), line congestion, operation cost, and carbon emission in the integrated power and transport systems is investigated.
- A multi-objective two-stage stochastic UC optimization problem incorporated with the VRP-based BESTrain model is proposed to minimize the operation cost and carbon emission simultaneously by considering wind energy and power demand uncertainties in real-time.

The remainder of the paper is organized as follows. In Section 2, the problem description containing RTN and the BESTrain model are presented. Section 3 represents the multi-objective two-stage stochastic UC formulation contains objective functions and corresponding restrictions. The solution method to solve the proposed multi-objective problem is described in Section 4. Numerical results are reported and discussed in Section 5. Finally, Section 6 concludes the paper.

2. Railway transport network and BESTrain

Railways are s safe land transport networks in the world for the daily movement of passengers or various objects. However, daily passenger transportation needs optimum scheduling for trains via a classic VRP model. Meanwhile, the BESTrain model through RTN needs more realistic modeling, by considering all transportation limitations, including rail station and railway conditions. The time-span network developed in [17], is implemented to model the railway stations and lines via VRP. Fig. 1 depicts a simple RTN network contains three train stations and railroads crossing. There are three neighboring stations $\{1,2,3\}$ in Fig. 1, in which the number on each line that links two stations together denotes the travel time, stated in time spans. One time-span can be each number of periods stated as an input to RTN. In Fig. 1, the travel time between stations 3 and 1 is two time-spans and twice other stations. To alleviate the problem, a virtual

station 4 is considered between stations 3 and 1; hence, the travel times between any two other stations equals a time span. The travel time, which is considered between any two stations in Fig. 1, is an important parameter in RTN. A small time span increases the elaboration of the RTN model with the assigned of different virtual stations, while a large time span will diminish the punctuality of the RTN modeling.

The TSN for 4 stations is depicted in Fig. 2. All available hourly interconnections between the actual and virtual stations are given in Fig. 2. The vertical axis shows railway stations, and the horizontal axis denotes the hourly scheduling horizon. Nodes and arcs are two main components in TSN. Each node shows a railway station (virtual or real station) in the scheduling horizon, and an arc expresses a possible connection between two stations or connection between stations and power network in the given time horizon. *Transporting arc* (dashed line) and *grid connecting arc* (solid line) are defined as two kinds of arcs in a TSN. *Grid connecting arc* shows the BESTrain stop for power exchanged with the power network at each station. *Transporting arc* demonstrates the BESTrain transportation between stations in each given time period. It is clear that the actual stations can be connected to both *transporting arcs* and *grid connecting*, but the virtual station (station 4 in Fig. 1) can only be connected to *transporting arcs*. Discernibly, the BESTrain could not be connected to the grid in station number 4 because of the absence of charging/discharging devices.

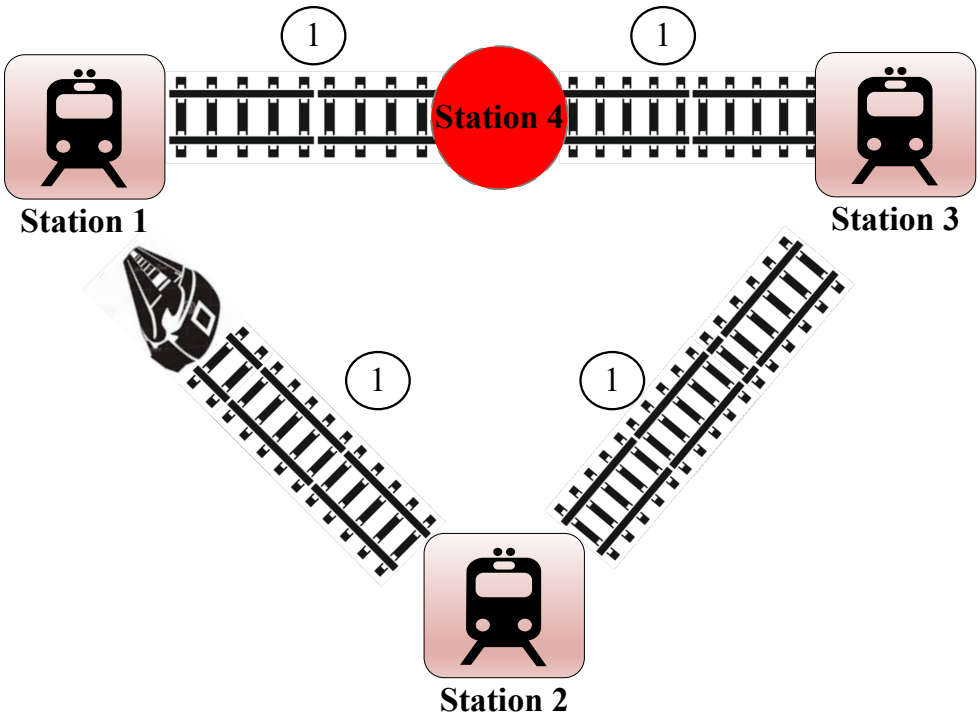

Fig. 1. The RTN structure.

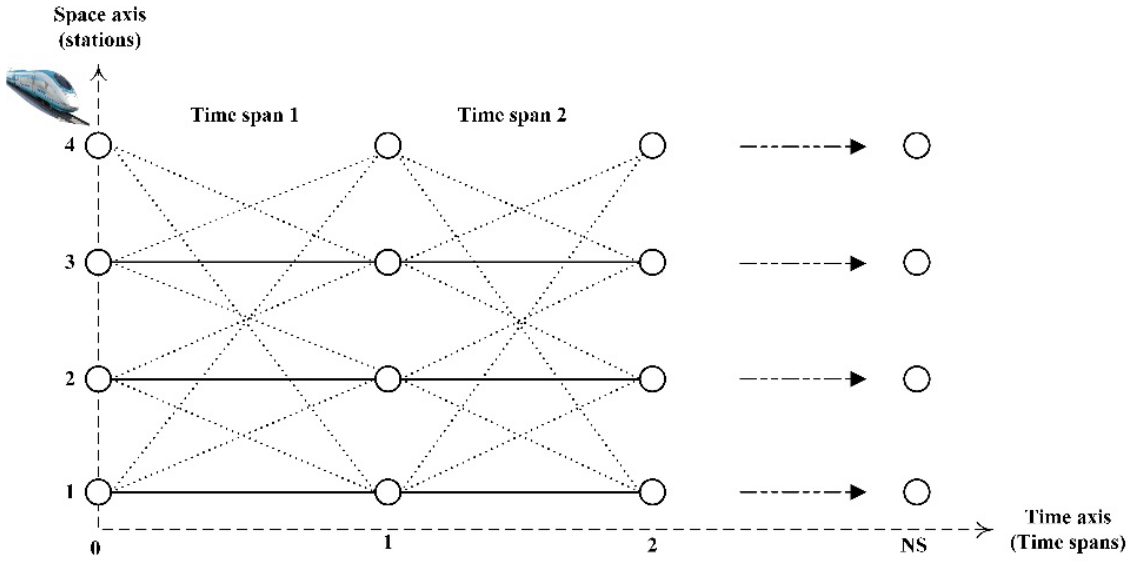

Fig. 2. TSN of example RTN structure.

3. Problem formulation

Fig. 3 depicts the overall schematic of the proposed multi-objective two-stage stochastic UC model in incorporation with VRP. In the proposed model, the ISO receives offers from power plants and BESTrain before solving the UC problem. The ISO prefers to utilize both production and demand-side sources to

realize the cost-effective hourly commitment of power plants. The BESTrain can be scheduled as a producer or consumer based on the ISO's requirements. The offered package of conventional power plants and BESTrain not only includes submitted price-quantity values but also includes their environmental and technical characteristics. As the VRP is combined with the UC problem, the ISO solves a UC problem limited to the RTN and power grid to minimize the operation cost and carbon emission under a multi-objective two-stage stochastic technique.

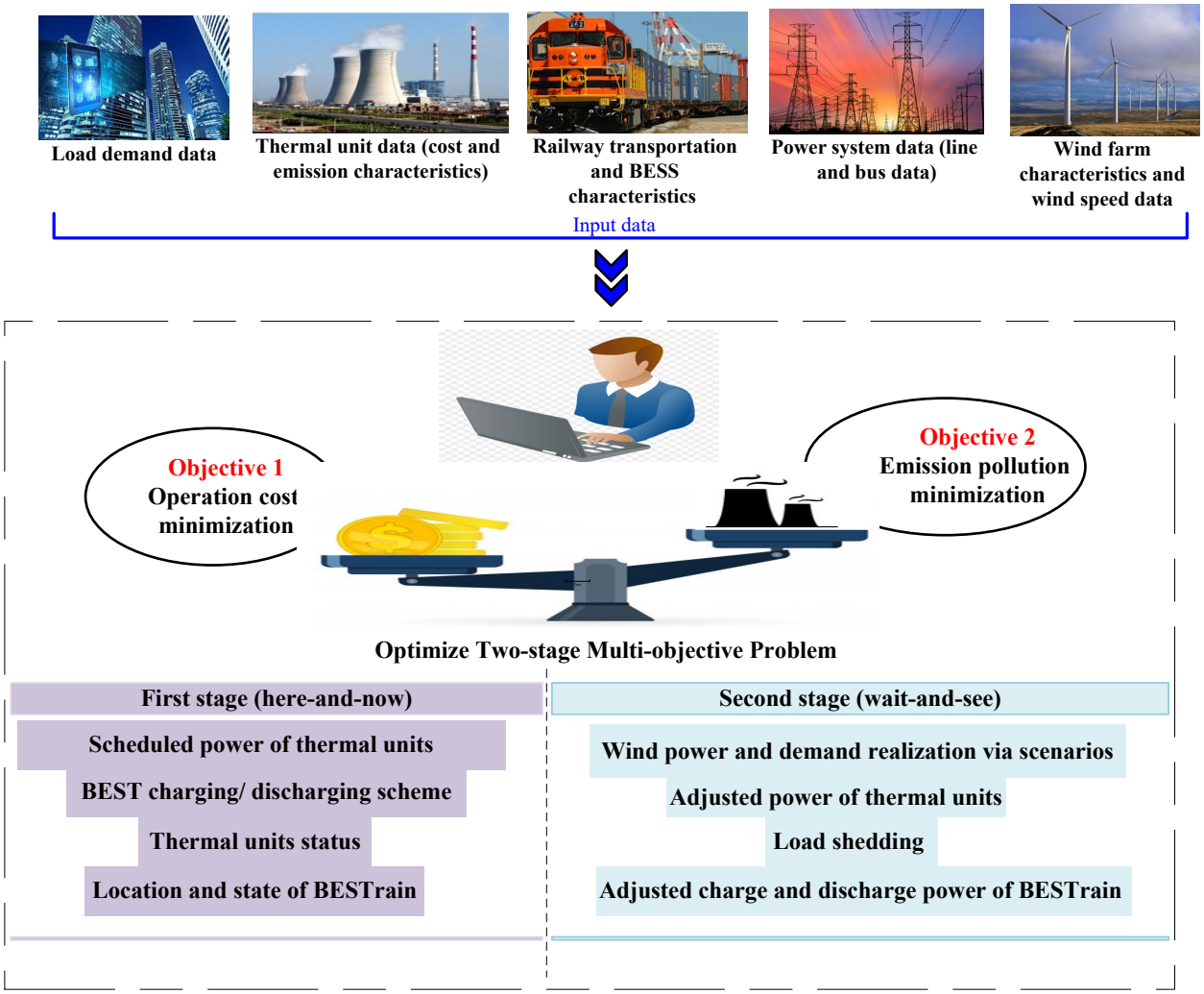

Fig. 3. The schematic of the proposed two-stage framework

The main objective of the proposed model is to minimize the carbon emission and total operational cost simultaneously, which is formulated as a multi-objective two-stage stochastic programming model to address the uncertainties associated with wind power production and electric demands in real-time. The objective function related to minimizing the total operating cost is defined as (1). The operational costs of

power plants in the first stage include the costs of no-load, start-up, and shut-down, as well as energy production costs, which are expressed by the first term of (1). The second term of (1) indicates transporting cost and charging and discharging costs of BESTrain in the first stage. It is assumed that the discharge/charge cost of BESTrain is a linear function of its discharge/charge energy [17]. In addition, the transportation cost of BESTrain is taken into account due to the train's fuel consumption on the way [17, 20]. The operational costs of power plants and BESTrain, as well as the cost of load shedding in the second stage, are provided by the third, fourth, and fifth terms of (1), respectively. The objective function related to minimizing carbon emission is represented by (2). The objective function (2) consists of three terms. The first and second terms of (2) show the carbon emission of power plants in the first stage. The carbon emission of power plants in the second stage is defined by the third term of (2).

$$\begin{aligned} OF_1 = \min & \sum_{t=1}^{T}\sum_{i=1}^{U}\left[MC_{i,t}I_{i,t} + SUC_{i,t} + SDC_{i,t} + \sum_{m=1}^{M} C_{i,t,m}^{E} P_{i,t,m} \right] \\ & + \sum_{tr=1}^{TR}\left[\sum_{(k,n)\in A}\sum_{ts=1}^{TS} C_{tr} I_{tr,k,n,ts} + \sum_{t=1}^{T}\left(C_{tr}^{C} P_{tr,t}^{C} + C_{tr}^{D} P_{tr,t}^{D} \right) \right] \\ & + \sum_{t=1}^{T}\sum_{s=1}^{S}\pi_s \left[\begin{array}{l} \sum_{i=1}^{U}\sum_{m=1}^{M} C_{i,t,m}^{E} \Delta P_{i,t,m,s} \\ + \sum_{tr=1}^{TR}\left(C_{tr}^{C} \Delta P_{tr,t,s}^{C} + C_{tr}^{D} \Delta P_{tr,t,s}^{D} \right) \\ + \sum_{j=1}^{NJ} voll_{j,t}\, Lsh_{j,t,s} \end{array} \right] \end{aligned} \tag{1}$$

$$OF_2 = \min \sum_{t=1}^{T}\sum_{i=1}^{U}\left[ME_{i,t} I_{i,t} + CE_{i,t} PE_{i,t} + \sum_{s=1}^{S} \pi_s CE_{i,t} \Delta PE_{i,t,s} \right] \tag{2}$$

1) First stage constraints

The set of limitations that must be satisfied in the first stage includes UC, BESTrain model, and power grid limitations. The set of constraints related to UC in the first stage is represented by (3) -(14) [36]. Constraints (3) and (4) shows the hourly power generation by the power plants. The up and down ramp rate limits for continuous times are expressed in (5) -(8), respectively. Minimum up and downtimes limitations of power

plants are defined by (9) -(12). The start-up and shut-down costs constraints are established by (11) and (12), respectively.

$$P_{i,m}^{\min} I_{i,t} \le P_{i,t,m} \le P_{i,m}^{\max} I_{i,t} \tag{3}$$

$$P_{i,t} = \sum_{m=1}^{M} P_{i,t,m} \tag{4}$$

$$P_{i,t} - P_{i,t\text{-}1} \le (1 - Y_{i,t}) R_i^{up} + Y_{i,t} P_i^{\min} \tag{5}$$

$$P_{i,t\text{-}1} - P_{i,t} \le (1 - Z_{i,t}) R_i^{dn} + Z_{i,t} P_i^{\min} \tag{6}$$

$$I_{i,t} - I_{i,t-1} = Y_{i,t} - Z_{i,t} \tag{7}$$

$$Y_{i,t} + Z_{i,t} \ge 1 \tag{8}$$

$$I_{i,t+TU_{i,u}} \ge I_{i,t} - I_{i,t-1} \tag{9}$$

$$TU_{i,u} = \begin{cases} u & u \le MUT_i \\ 0 & u > MUT_i \end{cases} \tag{10}$$

$$1 - I_{i,t+TD_{i,u}} \ge I_{i,t-1} - I_{i,t} \tag{11}$$

$$TD_{i,u} = \begin{cases} u & u \le MDT_i \\ 0 & u > MDT_i \end{cases} \tag{12}$$

$$\begin{aligned} &SU_{i,t} \ge C_i^{SU} (I_{i,t} - I_{i,t\text{-}1}) \\ &SU_{i,t} \ge 0 \end{aligned} \tag{13}$$

$$\begin{aligned} &SD_{i,t} \ge C_i^{SD} (I_{i,t-1} - I_{i,t}) \\ &SD_{i,t} \ge 0 \end{aligned} \tag{14}$$

The set of limitations associated with the operation of the BESTrain are expressed by (15) -(23) in the first stage [37]. The restriction related to the location of the BESTrain is represented by (15). Each train can be only on one route at any specified time span. Movement constraints for the BESTrain are expressed in (16) -(18). Let's consider the location of BESTrain at time span *s* in specific routes ending in the *k* node*;* hence at time span *s+1*, the BESTrain will be located in another route that starts from the *k* node, as expressed in (16). The final and initial states of the BESTrain location limits are represented by (17) and (18), respectively. At a special moment, the BESTrain can be operated in one of the charging or discharging modes when it is connected to the network, as represented by (19). The charged and discharged power constraints for the BEST are given by (20) -(21). The state of charge (SoC) of BESTrain is defined in (22).

BESTrain's energy capacity is restricted by min and max values as (23). The initial and final SoC for the BESTrain is limited to the constraint (24).

$$\sum_{(k,n)\in A} F_{tr,k,n,ts} = 1 \tag{15}$$

$$\sum_{(k,n)\in A_k^+} F_{tr,k,n,ts+1} = \sum_{(k,n)\in A_k^-} F_{tr,k,n,ts} \tag{16}$$

$$\sum_{(k,n)\in A_k^+} F_{tr,k,n,1} = F_{tr,k,0} \tag{17}$$

$$\sum_{(k,n)\in A_k^-} F_{tr,k,n,TS} = F_{tr,k,TS} \tag{18}$$

$$I_{tr,t}^{ch} + I_{tr,t}^{dis} \le F_{tr,k,k,ts} \tag{19}$$

$$P_{tr}^{ch,\min} I_{tr,t}^{ch} \le P_{tr,t}^{ch} \le P_{tr}^{ch,\max} I_{tr,t}^{ch} \tag{20}$$

$$P_{tr}^{dis,\min} I_{tr,t}^{dis} \le P_{tr,t}^{dis} \le P_{tr}^{dis,\max} I_{tr,t}^{dis} \tag{21}$$

$$E_{tr,t} = E_{tr,t-1} + \eta_{tr}^{ch} P_{tr,t}^{ch} - \frac{P_{tr,t}^{dis}}{\eta_{tr}^{dis}} \tag{22}$$

$$E_{tr}^{\min} \le E_{tr,t} \le E_{tr}^{\max} \tag{23}$$

$$E_{tr,0} = E_{tr,T} \tag{24}$$

The power balance and DC power flow limitations in the first stage are represented by (25) -(27) [38]. Constraint (25) expresses the power balance on each bus. The DC power flow equation is applied by (26). The thermal limit capacity for the transmission line is defined by (27).

$$\sum_{i=1}^{U_b} P_{i,t} + \sum_{wp=1}^{WP_b} P_{wp,t} + \sum_{tr=1}^{TR_b} \left[P_{tr,t}^{dis} - P_{tr,t}^{ch} \right] - \sum_{j=1}^{J_b} D_{j,t} = \sum_{i=1}^{U_b} PF_{b,b',t} \tag{25}$$

$$PF_{b,b',t} = \frac{\theta_{b,t} - \theta_{b',t}}{X_{b,b'}} \tag{26}$$

$$-PF_{Line}^{\max} \le PF_{b,b',t} \le PF_{Line}^{\max} \tag{27}$$

2) Second Stage Constraints

Constraints related to the second stage and "*wait and see*" variables are represented in this sub-section. The limitations of the power plants operating in the second stage are described by (28) -(32), including the power generation and ramp rate limits.

$$P^{r}_{i,t,s} = P_{i,t} + \Delta P_{i,t,s} \tag{28}$$

$$P^{\min}_{i,m} I_{i,t} \le P^{r}_{i,t,m,s} \le P^{\max}_{i,m} I_{i,t} \tag{29}$$

$$P^{r}_{i,t,s} = \sum_{m=1}^{M} P^{r}_{i,t,m,s} \tag{30}$$

$$P^{r}_{i,t,s} - P^{r}_{i,t-1,s} \le (1 - Y_{i,t}) R^{up}_{i} + Y_{i,t} P^{\min}_{i} \tag{31}$$

$$P^{r}_{i,t-1,s} - P^{r}_{i,t,s} \le (1 - Z_{i,t}) R^{dn}_{i} + Z_{i,t} P^{\min}_{i} \tag{32}$$

The BESTrain model limitations in the second stage are expressed by (33)-(39). The real charged and discharged power value of BESTrain are calculated in (33) and (34), respectively. The charge and discharge power limits in the second stage are respectively represented by (35) and (36). The limitations associated with the energy capacity limits related to the BESTrain for this stage are provided in (37) -(39).

$$P^{ch,r}_{tr,t,s} = P^{ch}_{tr,t} + \Delta P^{ch}_{tr,t,s} \tag{33}$$

$$P^{dis,r}_{tr,t,s} = P^{dis}_{tr,t} + \Delta P^{dis}_{tr,t,s} \tag{34}$$

$$P^{ch,\min}_{tr} I^{ch}_{tr,t} \le P^{ch,r}_{tr,t,s} \le P^{ch,\max}_{tr} I^{ch}_{tr,t} \tag{35}$$

$$E^{r}_{tr,t,s} = E^{r}_{tr,t-1,s} + \eta^{ch}_{tr} P^{ch,r}_{tr,t,s} - \frac{P^{dis,r}_{tr,t,s}}{\eta^{dis}_{tr}} \tag{37}$$

$$E^{\min}_{tr} \le E^{r}_{tr,t,s} \le E^{\max}_{tr} \tag{38}$$

$$E^{r}_{tr,0,s} = E^{r}_{tr,T,s} \tag{39}$$

Similar to the power flow and power balance constraints in the first stage, the network's limitations in the second stage should be established. The power balance restriction in the second stage is established by (40). The DC power flow and line power capacity limitation for the second stage are respectively defined by (41) and (42).

$$\sum_{i=1}^{U_b} P^{r}_{i,t,s} + \sum_{wp=1}^{WP_b} P^{r}_{wp,t,s} + \sum_{tr=1}^{TR_b} \left[P^{dis,r}_{tr,t,s} - P^{ch,r}_{tr,t,s} \right] - \sum_{j=1}^{J_b} D^{r}_{j,t,s} = \sum_{b=1}^{B} PF^{r}_{b,b',t,s} \tag{40}$$

$$PF^{r}_{b,b',t,s} = \frac{\theta^{r}_{b,t,s} - \theta^{r}_{b',t,s}}{X_{b,b'}} \tag{41}$$

$$-PF^{\max}_{Line} \le PF^{r}_{b,b',t,s} \le PF^{\max}_{Line} \tag{42}$$

4. SOLUTION METHOD: Ɛ-CONSTRAINT APPROACH

The UC model integrated with VRP is formulated as a multi-objective optimization problem to minimize the operation cost and carbon emission at the same time. The ε -constraint approach is introduced to solve the suggested multi-objective problem [39], which is described as following. Considering an optimization problem that contains n conflicting objectives and the corresponding limitation as (43):

$$\begin{aligned} W = \ & \min\{f_1(x), f_2(x), f_2(x), ..., f_n(x)\} \\ & \text{Subject to:} \\ & x \in R \end{aligned} \tag{43}$$

Where R is defined as a feasible region for the multi-objective approach and x is considered as a set of decision variables in the introduced problem. In this approach, one of the objectives is considered as the main objective, and others are included as constraints. Hence, by applying the Ɛ-constraint, the multi-objective problem in (43) is transferred to (44):

$$\begin{aligned} W = \ & \min f_1(x) \\ & \text{Subject to:} \\ & f_2(x) \le \varepsilon_2 \\ & f_3(x) \le \varepsilon_3 \\ & \vdots \\ & f_n(x) \le \varepsilon_n \\ & x \in R \end{aligned} \tag{44}$$

The members of Ɛ-set: $\{\varepsilon_2, \varepsilon_3, \varepsilon_4, ..., \varepsilon_k\}$, are adjusted parametrically to obtain the best optimal solutions. The optimal solutions of Ɛ-set are obtained according to the n-1 objective functions. Different strategies are applied to determine a compromise solution in a set of the provided Pareto solutions. The fuzzy-based decision-making approach is one of the appropriate options to achieve the best compromise solution among all possible solutions in the set of Pareto [40]. Based on this approach, the membership function in the range

[0,1] is assigned to all possible solutions in the Pareto set. In addition, for all of the objectives in (44), the fuzzy membership is provided as (45).

$$\hat{f}_k = \begin{cases} 1 & f_n \le f_n^L \\ \dfrac{f_n^{\max} - f_n}{f_n^{\max} - f_n^{\min}} & f_n^L \le f_n \le f_n^u \\ 0 & f_n \ge f_n^u \end{cases} \tag{45}$$

To designate the best reconciliation between generated solutions in the Pareto set, the min-max approach is applied based on calculating the smallest amounts of f_1 and f_2, and choosing the optimal solutions as a max amount of minimum $\left\{\hat{f}_1, \hat{f}_2\right\}$. More details can be found in [29, 41]. Fig. 4 shows the overall schematic of the proposed multi-objective UC model of power system with the RTN, based on the fuzzy-based decision-making strategy.

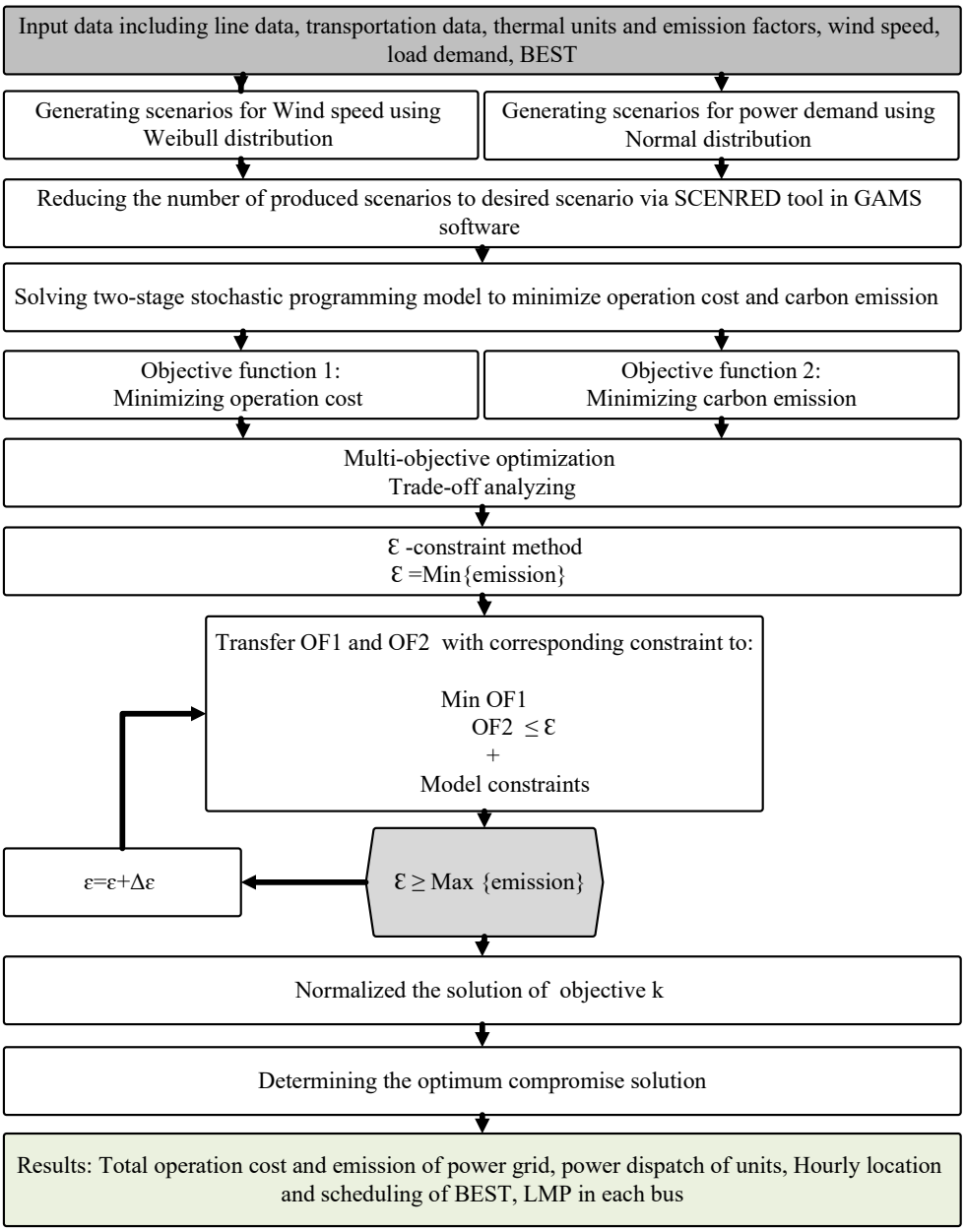

Fig. 4. The flowchart of the proposed multi-objective stochastic UC.

5. Case study and numerical results

1) Input data

In this research, a linked power and rail transport network is considered as Fig. 5 to analyze the performance of the presented model. All characteristics related to the power and transport networks are provided by [17]. The maximum capacity of line 1-4 (between buses 1 and 4) is assumed to be 105MW. The forecasted load and wind energy are given in Fig. 6. Also, the carbon emission coefficients and other characteristics related

to power plants can be found in [40, 42]. Unit G1 offers its power to market at three blocks as $13.51, $14.39, and $15.27, respectively. Unit G2 also offers its power to market at three blocks as $32.62, $32.71, and $32.83, respectively. In addition, unit G3 offers its power to market at three blocks as $17.7, $17.8, and $17.9, respectively. The carbon emission coefficient of units G1, G2, and G3 are considered to be 353.2 Ibs/MWh, 129.97 Ibs/MWh, and 137.41 Ibs/MWh, respectively. The cost of load shedding is assumed to be $400/MWh [43]. The proposed BESTrain is equipped with the sodium-sulfur (NaS) battery. The energy capacity, as well as the rated power of batteries, are 200 Wh/kg, and 50 W/Kg, respectively. Also, a standard 50-feet railway is applied to carry 100 tons of burden; hence, each wagon transfers NaS batteries with $100\times10^{3}\times200\times10^{-6}$ =20 MWh capacity and $100 \times 10^{3} \times 50\times 10^{-6}$ = 5MW power. The BESTrain includes six railroad wagons and a locomotive. As a result, the power and energy capacity characteristics of the BESTrain are 30 MW and 120 MWh, respectively. There is a 2-hours transport time between any two stations. The charge and discharge cost of BESTrain is estimated at 1$/MWh [44]. The transport cost of the BESTrain equals $200 [17]. Wind power and energy demand forecasting errors follow Weibull and normal distribution functions, respectively. The data relating to distribution functions are given in [45]. The 1000 scenarios are produced by the Monte-Carlo simulation, which are decreased to 10 probable scenarios by SCENRED. All the simulation and coding of the proposed MILP model is carried out in GAMS software and solved by CPLEX solver.

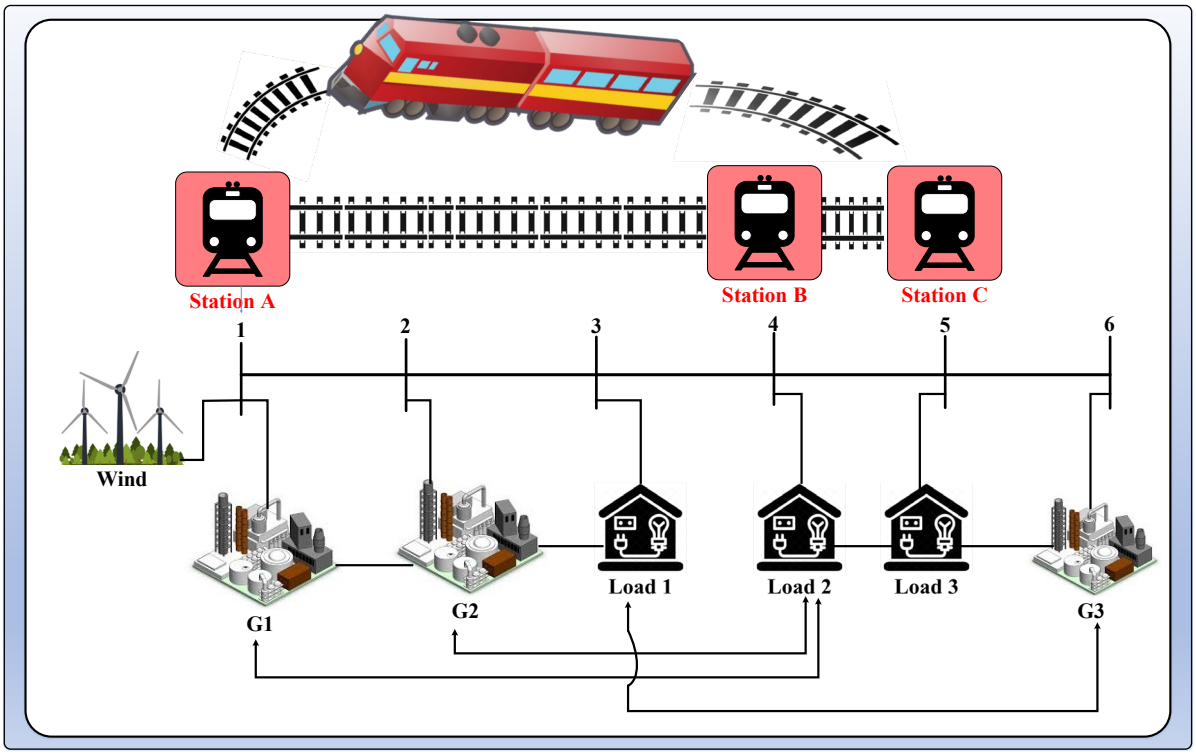

Fig. 5. The integrated power and RTN test system.

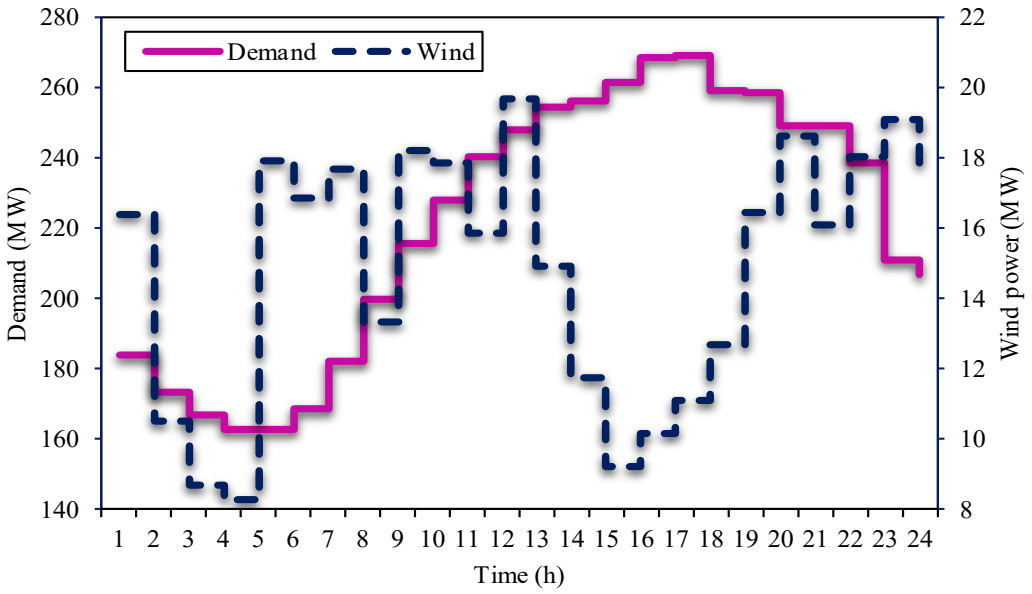

Fig. 6. The forecasted demand and wind power.

2) Numerical results

The following cases are studied to examine the effectiveness of the proposed model:

Case 1: Evaluating the effect of the static BESS in a single-objective two-stage UC to minimize the daily operation cost.

Case 2: Evaluating the impact of the BESTrain in a single-objective two-stage UC to minimize the daily operation cost.

Case 3: Evaluating the effect of the BESTrain in a multi-objective two-stage UC to minimize the daily operation cost and carbon emission.

Case 1: Fig. 7 shows the optimal charge and discharge scheme of the static BESS. It can be seen that for periods between 1 and 3, the BESS is operated in charging mode, then in the hours between 3 and 7, it is operated in discharging mode. The BESS cannot be used in discharge mode during hours of peak demand (t=15 to t=18) due to the congestion of lines, which results in the lack of optimal use of the potential of the BESS in reducing operating costs and the congestion of transmission lines during peak demand hours. Fig. 8 shows the hourly power dispatch of power plants with and without the BESS. Unit G1 is committed during the whole scheduling horizon as the cheapest power plants, and unit G3 is committed between hours 9 and 24 as a more expensive unit. Unit G2 is also operated between hours 10 and 23 as a high-cost power plant to supply the rest of the power demand. Besides, the BESS is only scheduled in such a way to manage the power dispatch of unit G1 more appropriately due to the congestion of lines during high-demand hours and its location on bus 1. Therefore, this leads to more efficient use of the generated power of unit G1. On the other hand, the BESS cannot be useful in reducing the power generation of units G2 and G3 due to line congestion, which leads to an insignificant decrease in total operating cost in the presence of the static BESS. The operating cost for this case is $86112.85, which is 0.9% less than it without the BESS.

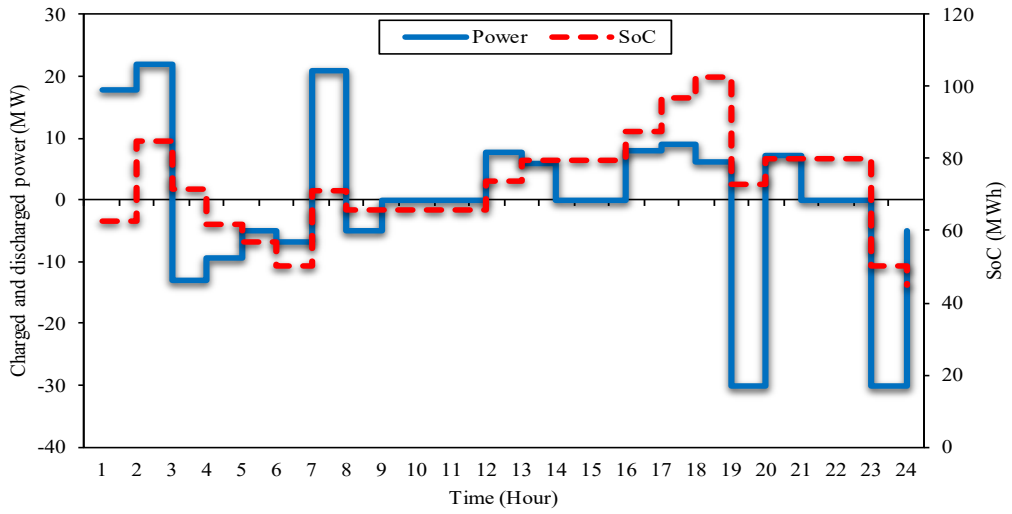

Fig. 7. The optimal charge and discharge scheme of the static BESS.

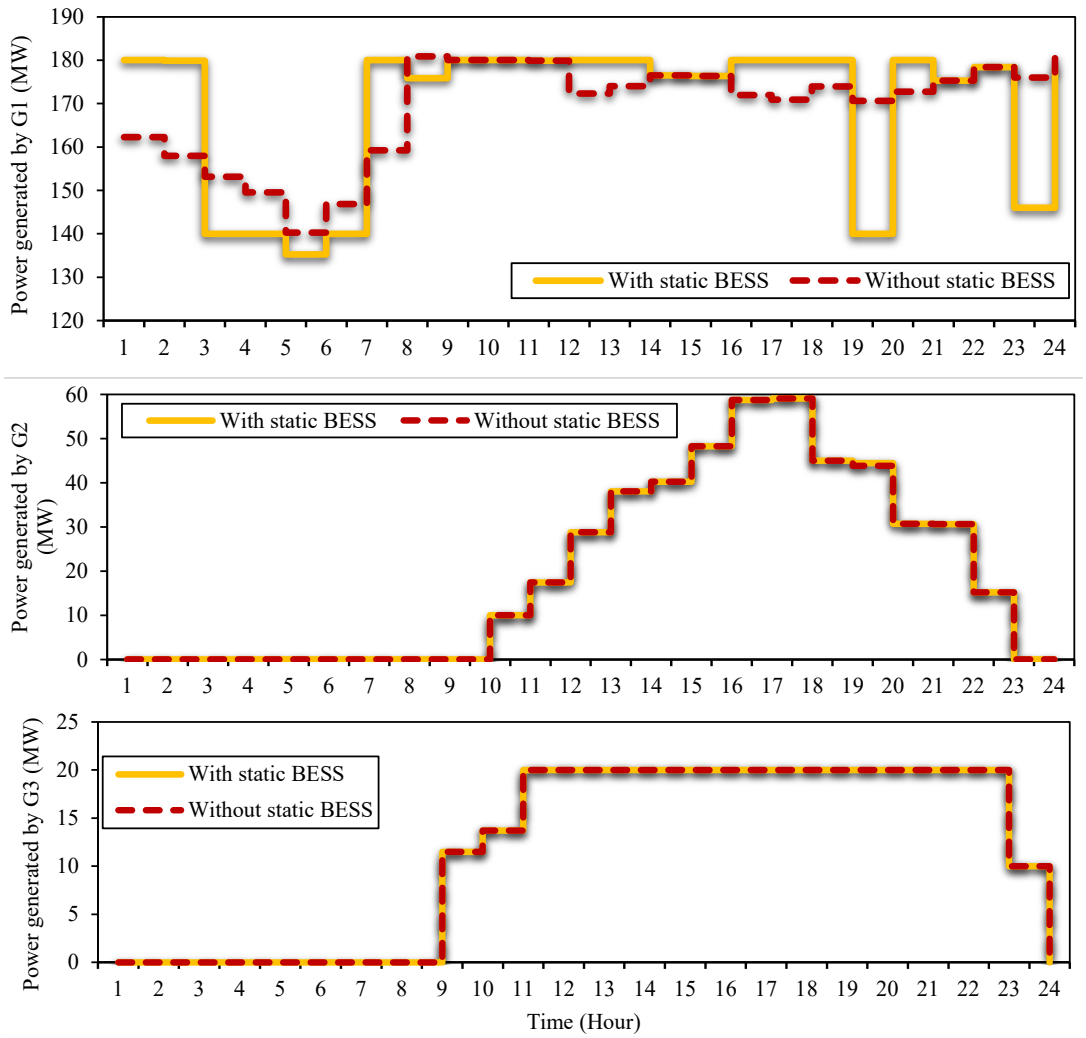

Fig. 8. The hourly power dispatch of power plants (G1, G2, and G3) with and without the BESS.

Case 2: The hourly location and status of the BESTrain is demonstrated in Table 1. The BESTrain is placed initially on station A. It is observed that in the first time-span, BESTrain departs from station A and moves to station B. From the second to the tenth time span, the BESTrain is placed on station B (fourth bus), and it is operated in charging and discharging modes to reduce the effect of line congestion during high-demand hours. In the eleventh time-span, BESTrain comes back to station A, and in the final time-span, BESTrain is operated in discharging and charging modes, respectively. The hourly scheduling of BESTrain is represented in Fig. 9. It is observed that during off-peak demand hours, the BESTrain is operated in charging mode to increase the state of charge of the battery. The BESTrain is operated in the discharge mode to follow the power demand and reduce power generation of units G2 and G3.

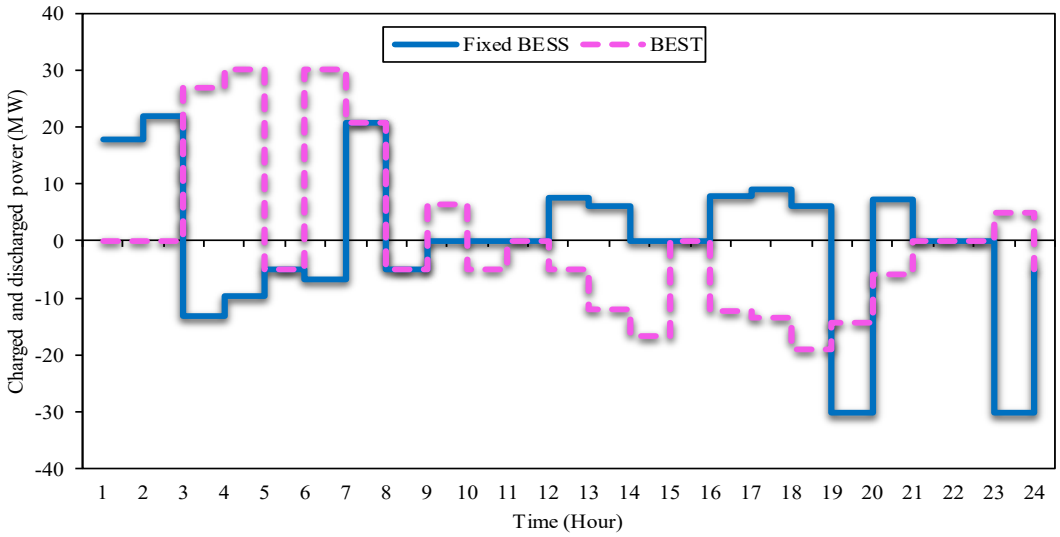

Fig. 9. Hourly charging and discharging scheme of BESTrain in Case 2.

In fact, during peak demand hours, the BESTrain can more effectively manage the effect of line congestion on power dispatch of unit G1 in comparison with the static BESS, as shown in more detail in Table 2 and Fig. 10. It is obvious from Table 2 that in low-demand hours, the power through the line 1-4 (between buses 1 and 4) is more when the BESTrain is operated instead of static BESS. Also, the power transmitted from the line 1-4 mainly is decreased in peak hours since the BESTrain is moved from station A (bus 1) to station B (bus 4) to relieve the impact of congestion of line 1-4 on the power dispatch of unit G1. At hours 15, 16, 20 and 21, although the maximum power is transmitted from the line 1-4, the power dispatch of unit G1 is increased by applying the BESTrain, which resulted in decreasing the participation of more expensive units (G2 and G3). Fig. 10 shows the hourly dispatch of units compared to case 1. It can be seen that the power generation of unit G1 significantly increases during peak hours in the presence of the BESTrain, which results in reducing power generation of units G2 and G3. Consequently, decrement of the power generation of units G2 and G3 and more efficient use of the power of the unit G1 in the presence of the BESTrain leads to a reduction in the average LMP during peak demand hours compared to case 1, which can be observed in Fig. 11. In this case, the daily operational cost equals $81,413.97, which is 5% less than case 1.

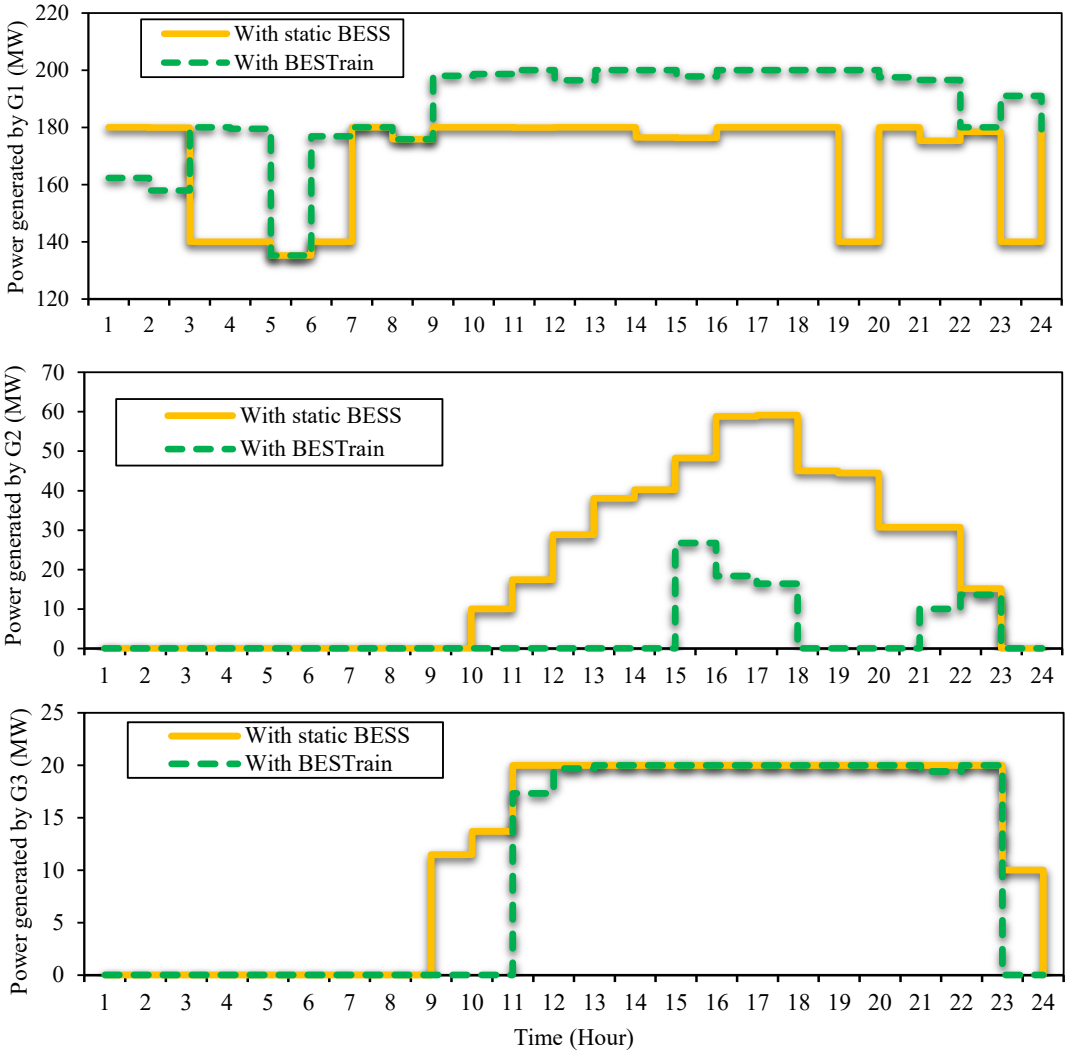

Fig. 10. The hourly power dispatch of power plants (G1, G2, and G3) for Case 2 in comparison with Case 1.

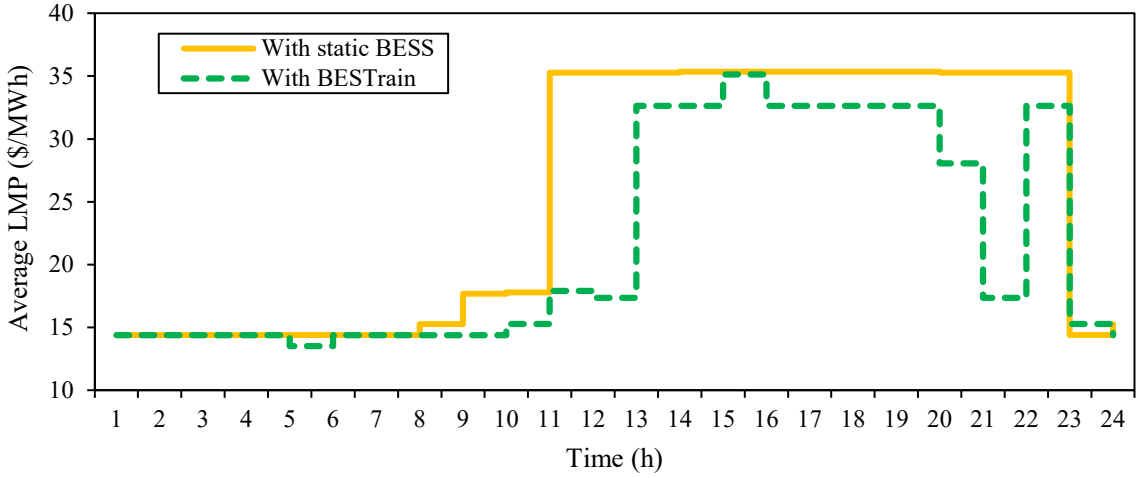

Fig. 11. The average value of LMP with static BESS and with the BESTrain.

Case 3: In this case, a multi-objective optimization problem is solved to minimize the operation cost and carbon emission simultaneously. Pareto's optimal solutions obtained from solving the multi-objective optimization problem without BESS, with static BESS, and with BESTrain are given in Figures 12-14, respectively. It can be seen that in all three Figures, by decreasing carbon emissions, the operation cost increases. This phenomenon reveals that to achieve lower carbon emissions, the operator should face a higher operating cost. The best solution among sets of Pareto's solutions is achieved using the fuzzy method, which without BESS, with the fixed BESS, and with BESTrain are obtained in iterations 10, 11, and 12, respectively. It can be observed that the best operational cost and carbon emission are obtained in the presence of BESS equal to $88350.03 and 34281.42 lbs, respectively, while these results without BESS equal to $ 88936.73 and $ 34758.87 lbs, respectively. Therefore, BESS reduces the operational cost and emission of carbon by 0.6% and 1.3%, respectively, compared to no BESS installation.

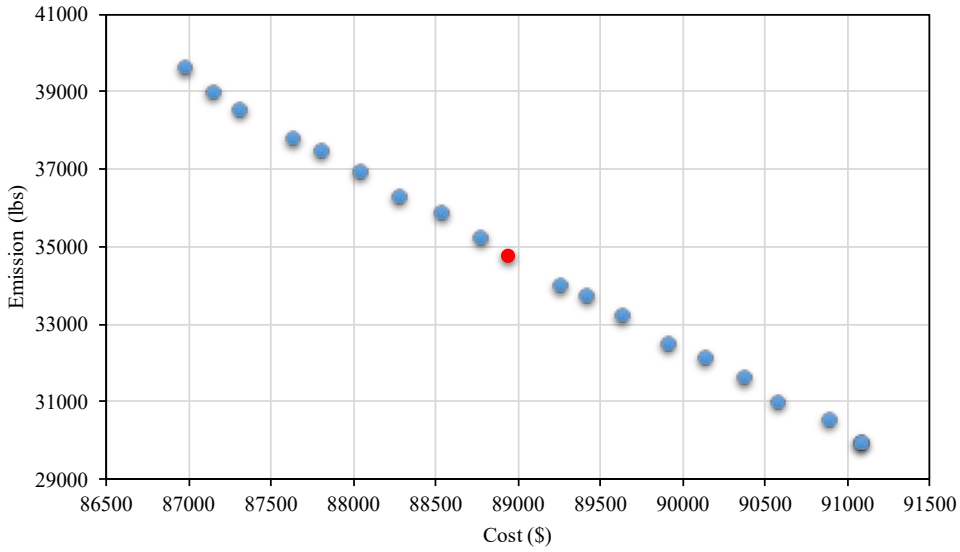

Fig. 12. Pareto's optimal solutions of the multi-objective optimization problem without BESS.

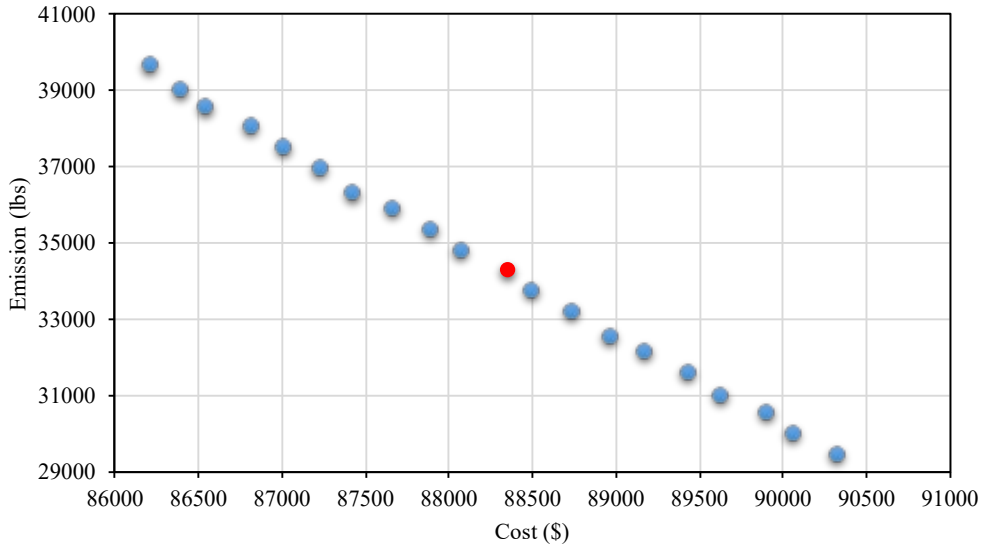

Fig. 13. Pareto's optimal solutions of the multi-objective optimization problem with BESS.

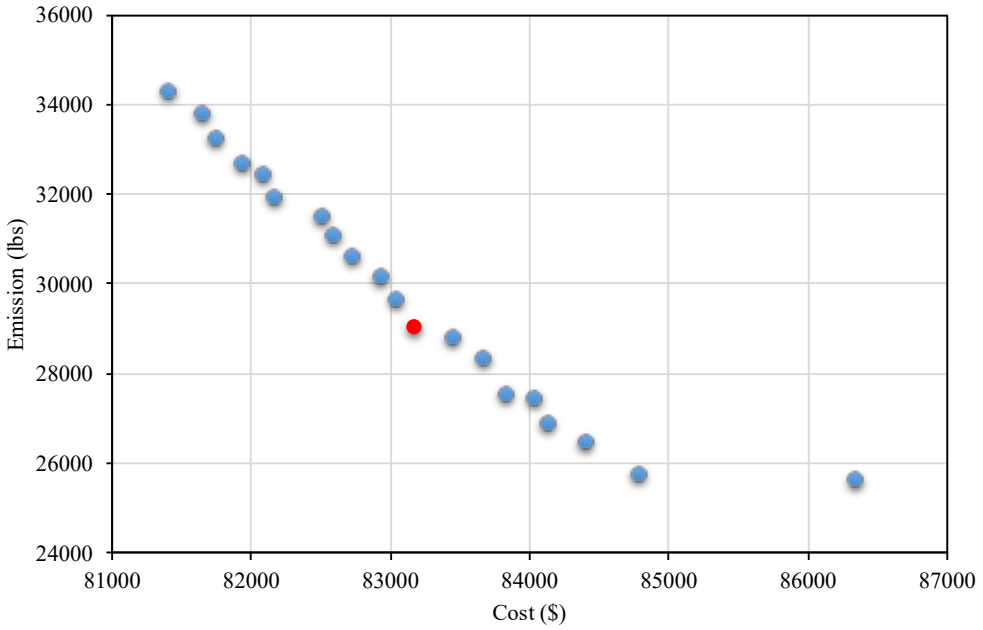

Fig. 14. Pareto's optimal solutions of the multi-objective optimization problem with BESTrain

Also, the best operation cost and carbon emission solutions are obtained in the presence of the BESTrain, which equals to $83169.27 and 29048.91 lbs, respectively, which leads to cost and carbon emission reduction by 6.2% and 18%, respectively, compared to the static BESS. These results confirm the potential of the BESTrain in the simultaneous reduction of the operational cost and carbon emission and the increment of the operator's decision-making flexibility. Figures 15 and 16 depict the effect of a multi-objective scheduling model on the power dispatch of units, as well as the optimal hourly scheme of

BESTrain, respectively. In peak hours, the power produced by G2 rises due to the lower carbon emissions than other units, which results in an increasing the total operational cost, consequently decreasing the daily carbon emission. Also, the optimal charge/discharge scheme of the BESTrain is dependent on the power generation by power plants. Therefore, the operator must apply a different operating strategy for the high-efficiency use of BESTrain under a multi-objective optimization approach.

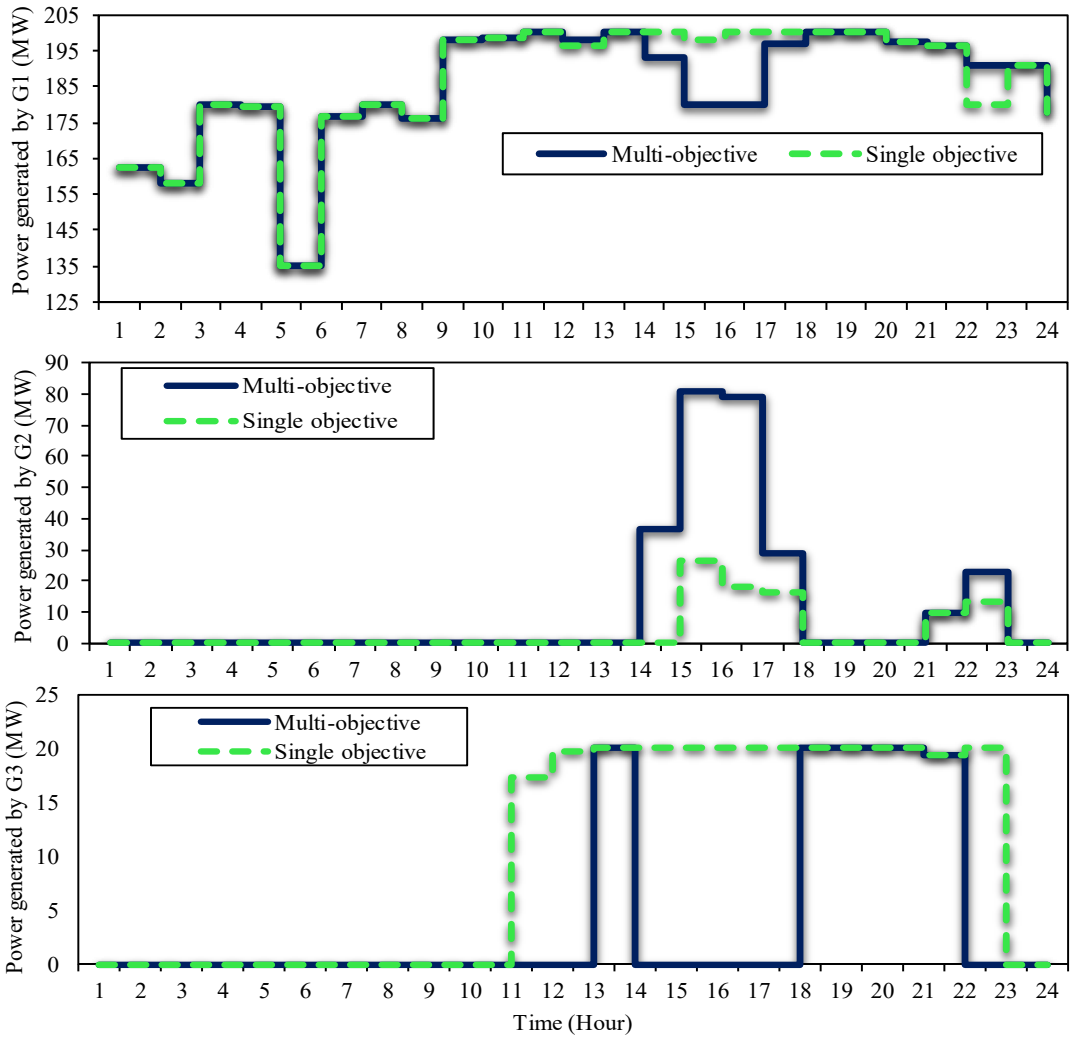

Fig. 15. The comparison of the hourly power dispatch of power plants (G1, G2, and G3) for single and multi-objective scheduling

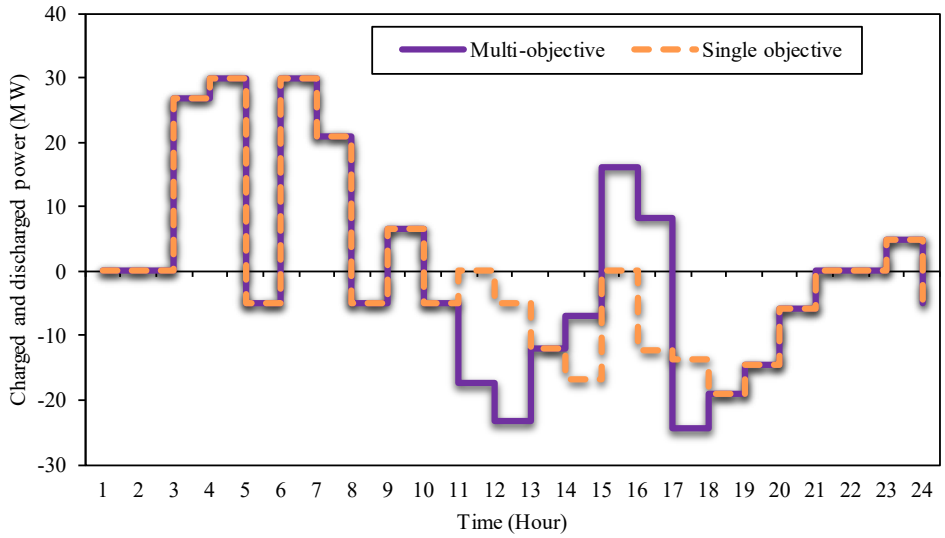

Fig. 16. Comparison of the hourly charging/ discharging scheme of the BESTrain for single and multi-objective optimization

Table 3 provides a comprehensive comparison between BESTrain and static BESS under different optimization approaches. It can be seen that in the single-objective scheduling model, BESTrain has a significant impact on the operation cost, leads to a reduction in the operation cost up to 6.5%. However, according to this table, the static BESS cannot be a very suitable option for the ISO to reduce the operation cost when the network faces the transmission lines congestion issue during peak hours. It can also be found that under the multi-objective optimization approach, the BESTrain acts as a much more suitable option to reduce operating costs and carbon emission compared to static BESS.

3) Discussion and main achievement

In the results section, three cases were considered to evaluate the performance of BESTrain in multi-objective UC, taking into account wind power and electricity demand uncertainties. In cases 1 and 2, we assessed the impact of static BESS and BESTrain from an economic and technical perspective, respectively. In case 3, we analyzed the static BESS and BESTrain from an economic and environmental perspective under a multi-objective optimization approach, where the objective was to minimize the operation cost and carbon emission simultaneously. The main achievements can be stated as follows:

- The operation cost was decreased by 0.6% in the presence of static BESS, while the BESTrain could reduce the total operation cost by 6.8%.

- The carbon emission was reduced by 1.3% in the presence of the static BESS, while applying BESTrain could lead to a decrease in the carbon emission by 19.3%.
- The static BESS could not significantly affect the reduction of transmission line congestion due to its low flexibility, while the BESTrain could reduce the transmission line congestion issue in peak hours by 10%.
- The average LMP was decreased by 8% in the presence of the BESTrain, while static BESS failed to reduce the average LMP due to line congestion issues in peak hours. The operation cost was decreased by 0.6% in the presence of static BESS, while the BESTrain could reduce the total operation cost by 6.8%.

6. Conclusion

This work investigated the technical, environmental, and economic influences of the BESTrain in a two-stage multi-objective UC model. To model the RTN and corresponding constraints, the time-space network was applied that linked the UC problem with the VRP. Besides, a two-stage scenario-based stochastic strategy was introduced to overcome the uncertainties caused by load and wind energy in real time. The presented model determined the power dispatch of power plants, the LMP in each bus, as well as hourly location and optimal charge/discharge schemes of the BESTrain by solving a multi-objective optimization problem. The optimal solution among all Pareto's solutions was determined using the fuzzy technique. The obtained results showed that the BESTrain could reduce the total operation cost and carbon emission by 6.8% and 19.3%, respectively. In contrast, the BESS could reduce the total operation cost and carbon emission by 0.6% and 1.3%, respectively.

The proposed model will be extended in our future works by considering the uncertainty related to forced outages of RTN and power system components under a contingency-based BESTrain UC model. Moreover, distributed optimization methods like the alternating direction method of multipliers will be applied in our future research to solve the model.

Reference

[1] "“Technology roadmap energy storage,” " *International Energy Agency,* 2014.
[2] X. Han, Z. Zhao, J. Li, and T. Ji, "Economic evaluation for wind power generation–hybrid energy storage system based on game theory," *International Journal of Energy Research,* vol. 41, pp. 49-62, 2017.
[3] P. Iliadis, S. Ntomalis, K. Atsonios, A. Nesiadis, N. Nikolopoulos, and P. Grammelis, "Energy management and techno-economic assessment of a predictive battery storage system applying a load levelling operational strategy in island systems," *International Journal of Energy Research,* vol. 45, pp. 2709-2727, 2021.
[4] N. V. Quynh, Z. M. Ali, M. M. Alhaider, A. Rezvani, and K. Suzuki, "Optimal energy management strategy for a renewable-based microgrid considering sizing of battery energy storage with control policies," *International Journal of Energy Research,* 2020.
[5] N. Li, C. Uckun, E. M. Constantinescu, J. R. Birge, K. W. Hedman, and A. Botterud, "Flexible operation of batteries in power system scheduling with renewable energy," *IEEE Transactions on Sustainable Energy,* vol. 7, pp. 685-696, 2015.
[6] A. Ahmadi, A. E. Nezhad, and B. Hredzak, "Security-constrained unit commitment in presence of lithium-ion battery storage units using information-gap decision theory," *IEEE Transactions on Industrial Informatics,* vol. 15, pp. 148-157, 2018.
[7] E. Heydarian-Forushani, M. E. H. Golshan, and P. Siano, "Evaluating the operational flexibility of generation mixture with an innovative techno-economic measure," *IEEE Transactions on Power Systems,* vol. 33, pp. 2205-2218, 2017.
[8] Z. Soltani, M. Ghaljehei, G. Gharehpetian, and H. Aalami, "Integration of smart grid technologies in stochastic multi-objective unit commitment: An economic emission analysis," *International Journal of Electrical Power & Energy Systems,* vol. 100, pp. 565-590, 2018.
[9] H. Chabok, M. Roustaei, M. Sheikh, and A. Kavousi-Fard, "On the assessment of the impact of a price-maker energy storage unit on the operation of power system: The ISO point of view," *Energy,* vol. 190, p. 116224, 2020.
[10] N. Hajibandeh, M. Shafie-khah, S. Talari, S. Dehghan, N. Amjady, S. J. Mariano*, et al.*, "Demand response-based operation model in electricity markets with high wind power penetration," *IEEE Transactions on sustainable Energy,* vol. 10, pp. 918-930, 2018.
[11] M. Sedighizadeh, M. Esmaili, and S. M. Mousavi-Taghiabadi, "Optimal energy and reserve scheduling for power systems considering frequency dynamics, energy storage systems and wind turbines," *Journal of Cleaner Production,* vol. 228, pp. 341-358, 2019.
[12] B. Wang, M. Zhou, B. Xin, X. Zhao, and J. Watada, "Analysis of operation cost and wind curtailment using multi-objective unit commitment with battery energy storage," *Energy,* vol. 178, pp. 101-114, 2019.
[13] P. P. Gupta, P. Jain, S. Sharma, K. C. Sharma, and R. Bhakar, "Stochastic scheduling of battery energy storage system for large-scale wind power penetration," *The Journal of Engineering,* vol. 2019, pp. 5028-5032, 2019.
[14] L. Alvarado-Barrios, Á. R. del Nozal, J. B. Valerino, I. G. Vera, and J. L. Martínez-Ramos, "Stochastic unit commitment in microgrids: Influence of the load forecasting error and the availability of energy storage," *Renewable Energy,* vol. 146, pp. 2060-2069, 2020.
[15] Y. Wen, C. Guo, H. Pandžić, and D. S. Kirschen, "Enhanced security-constrained unit commitment with emerging utility-scale energy storage," *IEEE Transactions on power Systems,* vol. 31, pp. 652-662, 2015.

[16] M. Joos and I. Staffell, "Short-term integration costs of variable renewable energy: Wind curtailment and balancing in Britain and Germany," *Renewable and Sustainable Energy Reviews,* vol. 86, pp. 45-65, 2018.
[17] Y. Sun, Z. Li, M. Shahidehpour, and B. Ai, "Battery-based energy storage transportation for enhancing power system economics and security," *IEEE Transactions on Smart Grid,* vol. 6, pp. 2395-2402, 2015.
[18] S. Yao, P. Wang, and T. Zhao, "Transportable energy storage for more resilient distribution systems with multiple microgrids," *IEEE Transactions on Smart Grid,* vol. 10, pp. 3331-3341, 2018.
[19] Y. Sun, Z. Li, W. Tian, and M. Shahidehpour, "A Lagrangian decomposition approach to energy storage transportation scheduling in power systems," *IEEE Transactions on Power Systems,* vol. 31, pp. 4348-4356, 2016.
[20] Y. Sun, J. Zhong, Z. Li, W. Tian, and M. Shahidehpour, "Stochastic scheduling of battery-based energy storage transportation system with the penetration of wind power," *IEEE Transactions on Sustainable Energy,* vol. 8, pp. 135-144, 2016.
[21] P. Prabawa and D.-H. Choi, "Multi-agent framework for service restoration in distribution systems with distributed generators and static/mobile energy storage systems," *IEEE Access,* vol. 8, pp. 51736-51752, 2020.
[22] H. Saboori and S. Jadid, "Optimal scheduling of mobile utility-scale battery energy storage systems in electric power distribution networks," *Journal of Energy Storage,* vol. 31, p. 101615, 2020.
[23] M. Ahrabi, M. Abedi, H. Nafisi, M. A. Mirzaei, B. Mohammadi-Ivatloo, and M. Marzband, "Evaluating the effect of electric vehicle parking lots in transmission-constrained AC unit commitment under a hybrid IGDT-stochastic approach," *International Journal of Electrical Power & Energy Systems,* vol. 125, p. 106546, 2021.
[24] M. E. Khodayar, L. Wu, and Z. Li, "Electric vehicle mobility in transmission-constrained hourly power generation scheduling," *IEEE Transactions on Smart Grid,* vol. 4, pp. 779-788, 2013.
[25] Y. Sun, Z. Chen, Z. Li, W. Tian, and M. Shahidehpour, "EV charging schedule in coupled constrained networks of transportation and power system," *IEEE Transactions on Smart Grid,* vol. 10, pp. 4706-4716, 2018.
[26] J. Atherton, R. Sharma, and J. Salgado, "Techno-economic analysis of energy storage systems for application in wind farms," *Energy,* vol. 135, pp. 540-552, 2017.
[27] T. Terlouw, T. AlSkaif, C. Bauer, and W. van Sark, "Multi-objective optimization of energy arbitrage in community energy storage systems using different battery technologies," *Applied Energy,* vol. 239, pp. 356-372, 2019.
[28] M. Sedighizadeh, M. Esmaili, A. Jamshidi, and M.-H. Ghaderi, "Stochastic multi-objective economic-environmental energy and reserve scheduling of microgrids considering battery energy storage system," *International Journal of Electrical Power & Energy Systems,* vol. 106, pp. 1-16, 2019.
[29] J. Aghaei and M.-I. Alizadeh, "Multi-objective self-scheduling of CHP (combined heat and power)-based microgrids considering demand response programs and ESSs (energy storage systems)," *Energy,* vol. 55, pp. 1044-1054, 2013.
[30] A. Abdon, X. Zhang, D. Parra, M. K. Patel, C. Bauer, and J. Worlitschek, "Techno-economic and environmental assessment of stationary electricity storage technologies for different time scales," *Energy,* vol. 139, pp. 1173-1187, 2017.

[31] R. Hemmati, "Technical and economic analysis of home energy management system incorporating small-scale wind turbine and battery energy storage system," *Journal of Cleaner Production,* vol. 159, pp. 106-118, 2017.
[32] B. Lokeshgupta and S. Sivasubramani, "Multi-objective home energy management with battery energy storage systems," *Sustainable Cities and Society,* vol. 47, p. 101458, 2019.
[33] L. Luo, S. S. Abdulkareem, A. Rezvani, M. R. Miveh, S. Samad, N. Aljojo*, et al.*, "Optimal scheduling of a renewable based microgrid considering photovoltaic system and battery energy storage under uncertainty," *Journal of Energy Storage,* vol. 28, p. 101306, 2020.
[34] M. Zolfaghari, N. Ghaffarzadeh, and A. J. Ardakani, "Optimal sizing of battery energy storage systems in off-grid micro grids using convex optimization," *Journal of Energy Storage,* vol. 23, pp. 44-56, 2019.
[35] H. Mehrjerdi and R. Hemmati, "Modeling and optimal scheduling of battery energy storage systems in electric power distribution networks," *Journal of Cleaner Production,* vol. 234, pp. 810-821, 2019.
[36] M. A. Mirzaei, M. Nazari-Heris, B. Mohammadi-Ivatloo, K. Zare, M. Marzband, M. Shafie-Khah*, et al.*, "Network-Constrained Joint Energy and Flexible Ramping Reserve Market Clearing of Power-and Heat-Based Energy Systems: A Two-Stage Hybrid IGDT–Stochastic Framework," *IEEE Systems Journal,* 2020.
[37] M. A. Mirzaei, M. Hemmati, K. Zare, B. Mohammadi-Ivatloo, M. Abapour, M. Marzband*, et al.*, "Two-stage robust-stochastic electricity market clearing considering mobile energy storage in rail transportation," *IEEE Access,* vol. 8, pp. 121780-121794, 2020.
[38] N. Nasiri, A. S. Yazdankhah, M. A. Mirzaei, A. Loni, B. Mohammadi-Ivatloo, K. Zare*, et al.*, "A bi-level market-clearing for coordinated regional-local multi-carrier systems in presence of energy storage technologies," *Sustainable Cities and Society,* vol. 63, p. 102439, 2020.
[39] M. Hemmati, M. A. Mirzaei, M. Abapour, K. Zare, B. Mohammadi-ivatloo, H. Mehrjerdi*, et al.*, "Economic-environmental analysis of combined heat and power-based reconfigurable microgrid integrated with multiple energy storage and demand response program," *Sustainable Cities and Society,* vol. 69, p. 102790, 2021.
[40] M. Nazari-Heris, M. A. Mirzaei, B. Mohammadi-Ivatloo, M. Marzband, and S. Asadi, "Economic-environmental effect of power to gas technology in coupled electricity and gas systems with price-responsive shiftable loads," *Journal of Cleaner Production,* vol. 244, p. 118769, 2020.
[41] M. Nazari-Heris, M. A. Mirzaei, B. Mohammadi-Ivatloo, M. Marzband, and S. Asadi, "Economic-environmental effect of power to gas technology in coupled electricity and gas systems with price-responsive shiftable loads," *Journal of Cleaner Production,* p. 118769, 2019.
[42] A. Alabdulwahab, A. Abusorrah, X. Zhang, and M. Shahidehpour, "Coordination of interdependent natural gas and electricity infrastructures for firming the variability of wind energy in stochastic day-ahead scheduling," *IEEE Transactions on Sustainable Energy,* vol. 6, pp. 606-615, 2015.
[43] M. A. Mirzaei, A. S. Yazdankhah, B. Mohammadi-Ivatloo, M. Marzband, M. Shafie-khah, and J. P. Catalão, "Stochastic network-constrained co-optimization of energy and reserve products in renewable energy integrated power and gas networks with energy storage system," *Journal of cleaner production,* vol. 223, pp. 747-758, 2019.

[44] M. Sadat-Mohammadi, M. Nazari-Heris, S. Asadi, and H. Jebelli, "An Incentive-Based Vehicle to Grid Service in Electrical Energy Networks Considering the Effect of Battery Degradation Cost," in *Construction Research Congress 2020: Infrastructure Systems and Sustainability*, 2020, pp. 314-321.
[45] M. Hemmati, B. Mohammadi-Ivatloo, M. Abapour, and A. Anvari-Moghaddam, "Optimal Chance-Constrained Scheduling of Reconfigurable Microgrids Considering Islanding Operation Constraints," *IEEE Systems Journal,* 2020.

Table 1. Status and location of the BESTrain

Daily operation cost= $81,413.97				
Time span	**1**	**2**	**3**	**4**
BESTrain location	A to B	B	B	B
BEST state	Transportation	-/Charge	Charging /Discharging	Charging
Time span	**5**	**6**	**7**	**8**
BESTrain location	B	B	B	B
BEST state	Discharging /Charging	Discharging	Discharging	Discharging
Time span	**9**	**10**	**11**	**12**
BESTrain location	B	B	B to A	A
BESTrain state	Discharging	Discharging	Transportation	Charge/Discharge

Table 2. The effect of BESTrain on the congestion of line 1-4

Time (h)	Hourly demand (MW)	Power flow of line 1-4 (MW)	
		Static BESS	BESTrain
1	183.949	86.676	86.676
2	173.407	81.709	81.709
3	166.603	78.503	92.081
4	162.467	76.553	91.726
5	162.813	76.717	74.188
6	168.504	79.398	94.571
7	182.059	85.785	96.296
8	199.92	94.201	91.672
9	215.838	101.702	105.000
10	228.06	98.643	104.932
11	240.04	104.939	104.939
12	247.905	104.130	105.000
13	254.289	105.000	104.274
14	255.78	105.000	102.641
15	261.303	105.000	105.000
16	268.58	105.000	105.000
17	268.8	105.000	104.881
18	259.077	105.000	103.050
19	258.269	105.000	104.963
20	249.217	105.000	105.000
21	249.175	105.000	105.000
22	238.497	103.260	98.512
23	211.103	94.756	99.470
24	206.588	97.343	97.343

Table 3. Comprehensive comparison of BESTrain with static BESS

Optimization model	**Single-objective (operation cost)**		**Multi-objective**	
Storage model	Static BESS	BESTrain	Static BESS	BESTrain
Operation cost ($)	86,112.85	81,413.97	88,350.03	83,169.27
Carbon emission (lbs)	-	-	34,281.42	29,048.91
Cost-saving compared without storage (%)	0.9	6.5	0.6	6.8